arXiv:2603.09813v1 [cs.CG] 10 Mar 2026

Prismatoid Band-Unfolding Revisited

Joseph O'Rourke*

March 11, 2026

Abstract

It remains unknown if every prismatoid has a nonoverlapping edge-unfolding, a special case of the long-unsolved "Dürer's problem." Recently nested prismatoids have been settled [Rad24] by mixing (in some sense) the two natural unfoldings, petal-unfolding and band-unfolding. Band-unfolding fails due to a specific counterexample [O'R13b].

The main contribution of this paper is a characterization when a band-unfolding of a nested prismatoid does in fact result in a nonoverlapping unfolding. In particular, we show that the mentioned counterexample is in a sense the only possible counterexample. Although this result does not expand the class of shapes known to have an edge-unfolding, its proof expands our understanding in several ways, developing tools that may help resolve the non-nested case.

1 Introduction

1.1 Background

The long-unsolved Dürer's problem asks if every convex polyhedron can be ***edge-unfolded*** to a single simple (non-self-overlapping) planar polygon [O'R13a].[1] Among the various special classes of polyhedra investigated are prismoids and prismatoids. A ***prismoid*** is the convex hull of two convex polygons in parallel planes, B the base below and A the top above, where A is angularly similar to B and aligned so the edges of A are parallel to the edges of B. The lateral faces of a prismoid are trapezoids. All prismoids are known to have an edge-unfolding.

A ***prismatoid*** is the convex hull of two convex polygons B and A in parallel planes with no restrictions on the shapes of B and A. This is a considerably wider class of polyhedra, and it remains open whether every prismatoid has an edge-unfolding.

	Lateral Faces	Edges	Vertices	Safe Cut (nested)?
Prismoid	trapezoids	parallel	$\lvert B\rvert = \lvert A\rvert$	$\exists$
Prismatoid	triangles	arbitrary	arbitrary	open

*Smith College, jorourke@smith.edu

[1] We'll use "edge-unfolding" to mean nonoverlapping, and "overlap" to mean strict overlap, sharing interior points.

There are two natural edge-unfolding approaches: a ***petal-unfolding***, where the lateral faces unfold splayed around B and A is attached at a petal tip, and a ***band-unfolding***, where the lateral faces L unfold to a strip with B and A attached to opposite sides. It is known that every topless prismatoid has a petal-unfolding, but unknown whether every prismatoid has a petal-unfolding [O'R13b]. An explicit counterexample for band-unfoldings for nested prismatoids was described in [O'R07].

In a ***nested prismatoid***, the top A projects orthogonally strictly into B. Recently it was proved that every nested prismatoid has an edge-unfolding [Rad24]. The proof uses a clever mix of petal-unfolding and band-unfolding. Whether non-nested prismatoids have an edge-unfolding remains open.

1.2 Results

The main contribution of this paper is a characterization when a band-unfolding of a nested prismatoid does in fact result in a nonoverlapping unfolding. In particular, we show that the counterexample in [O'R07]—see Fig. 1—is in a sense the only possible counterexample.

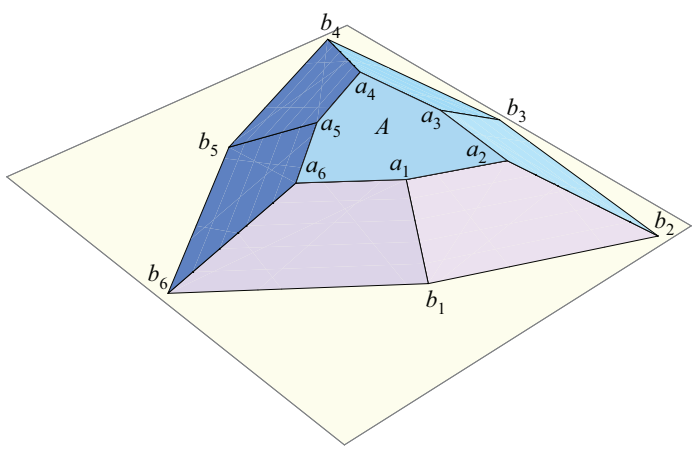

Figure 1: Hexagonal counterexample. Fig. 1 in [O'R13b].

More precisely, we prove this theorem:

Theorem 1 *Any nested prismatoid that satisfies these two constraints has a band edge-unfolding:*

(1) The top convex polygon A has the radial monotone (RM) property.

(2) The band L has a "safe cut" compatible with the RM-property.

with B and A attached to opposite sides of the cut-open band.

Although this theorem does not expand the class of shapes known to have an edge-unfolding (because [Rad24] settles nested prismatoids), it does expand our understanding in several ways:

(a) The band-unfolding counterexample was a "one-off" fact with no explanation. But now (1) of the theorem characterizes the shapes of A that accommodate band-unfolding.

(b) The proof starts with A pushed down to form a doubly-covered polyhedron, and lifts A to its z-height. This overall proof approach shows promise for resolving other shapes, perhaps including non-nested prismatoids.

(c) Several tools developed for the proof, including the opening lemmas in Section 3 (summarized in Theorem 2), may help in other proofs.

(d) The connection to radial monotonicity is novel, tying together Cauchy's arm lemma, the involute of a convex curve (Fig. 11), and the composition of planar rotations (Proposition 9).

(e) The proof handles all A z-heights at once.

Safe Cuts. A band L has a ***safe cut*** if there is an edge e such that cutting e unfolds the band without overlap, so is "safe." (Here B and A play no role.) Perhaps surprisingly, not every edge of L is a safe cut. We don't focus on safe cuts in this paper, but requirement (2) of the theorem needs safe cuts. It was shown in [ADL+08] by a difficult proof that nested prismoid bands do have a safe cut. Whether nested prismatoids have a safe cut is an interesting unsolved question.

2 Band-Unfolding: Overall Plan

The prismatoid P to be edge-unfolded consists of the base B in the xy-plane and the top $A = A_z$ above the base, $z > 0$. P is ***nested*** if $A_0 \subset B$.

The edges cut for the unfolding consist of

(1) Cut all but one edge of B.

(2) Cut all but one edge of A.

(3) Cut one lateral band edge connecting B to A, a safe cut.

The unfolding then consists of the band L, with B attached to the B-side of L and A to the A-side. See Fig. 2 for one example, and Section 6 for more examples.

Lifting A to $z > 0$. We now describe at a high level how an edge-unfolding is obtained for a given prismatoid P. Let the height of A be $z > 0$. We first project A down to $z = 0$ producing a doubly-covered polyhedron $\overline{P}$ in the xy-plane. The underside of $\overline{P}$ is B. The top side contains the band L_0 and A_0,

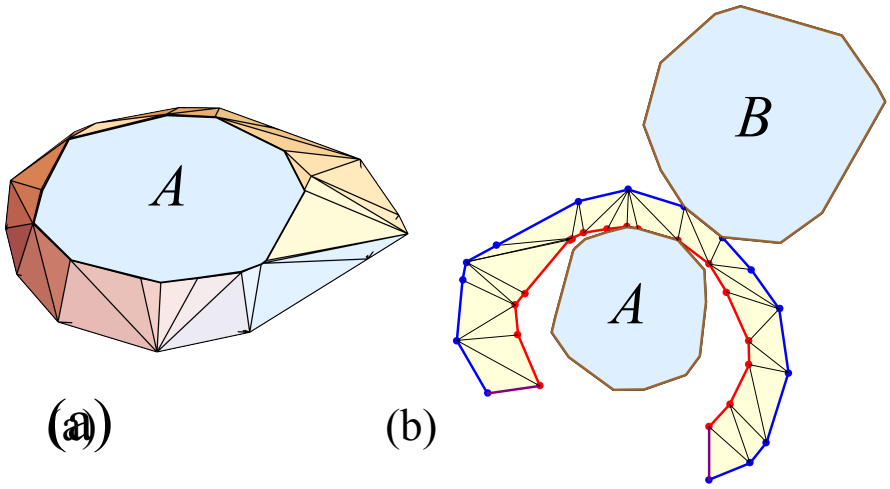

Figure 2: $n_B, n_A = 14, 16$. Here $z = 0.2$ when the diameter of B is 1.

with the subscript indicating $z = 0$. Note the shape of A is independent of z, while L_z depends on z.

Now we perform the cuts enumerated above on $\overline{P}$, with the uncut B and A attachment edges yet to be described. This allows B to flip out around its uncut edge, leaving a layout or development D_0 in the plane that does not self-overlap.

Finally we lift A_z to its original z-height, and open the L_B and L_A chains accordingly.. The opening straightens the band, and with careful placement of A attached to L_A, avoids overlap.

Although the argument only needs to consider the layout D_0 and D_z, it aids intuition to think of z changing continuously from $z = 0$ to arbitrarily high z, for all the intermediate shapes avoid overlap. (This continuous viewpoint is the only place that employs Lemma 4 below.)

3 Opening Lemmas

A key to the proof is that lifting A "opens" or "straightens" the band. This section proves the lemmas supporting this claim. Theorem 2 summarizes the lemmas. In some sense, Theorem 2 is obvious: just an application of the spherical triangle inequality. Radons Observation 2.2 [Rad24] calls opening "stretching," and leaves details unstated. One can view the lemmas in this section as formally proving those details.

Setup and Notation. Let a, b, c be three points in the xy-plane, and v a point above the plane, $v_z > 0$. We'll use cw for clockwise and ccw for counterclockwise throughout. Let the planar ccw angle at b be $\theta = \angle a, b, c \leq \pi$. We assume that v projects to the convex side, to v_0 in the xy-plane.

Form two triangles $\triangle abv$ and $\triangle bcv$; so edge vb is incident to b. See Fig. 3(a). Let ϕ be the sum of the two incident 3D angles at b:

$$\phi = \phi_a + \phi_c = \angle a, b, v + \angle v, b, c \ .$$

The claim of Lemma 1 is that ϕ is an ***opening*** of θ: $\pi \geq \phi > \theta$. For intuition, imagine lifting v_z from 0 toward $z = \infty$. Then angles ϕ_a and ϕ_c both approach $\pi/2$, and so ϕ approaches π. The situation is perhaps more delicate than it might initially appear, for it could be that ϕ_a increases to $\pi/2$ while ϕ_c decreases to $\pi/2$, and their sum increases to π.

Lemma 1 *Under the conditions just described, with planar convex angle* $0 < \theta \leq \pi$*, then for* $z > 0$*,* $\pi \geq \phi > \theta$*:* ϕ *is an opening of* θ*.*

Proof: The proof is established by the triangle inequality on the Gaussian sphere. Let $\mathbb{S}$ be the unit-radius sphere centered on the origin. Normalize the three vectors $\vec{a} = a - b$, $\vec{c} = c - b$, $\vec{v} = v - b$. The arc $\vec{a}\,\vec{c}$ has length θ. and similarly, the arcs $\vec{a}\,\vec{v}$ and $\vec{c}\,\vec{v}$ have lengths ϕ_a and ϕ_c respectively. See Fig. 3(b).

Then $\phi = \phi_a + \phi_c > \theta$ follows from the triangle inequality on the sphere. Only when v projects directly on b is $\phi = \pi$. Otherwise, ϕ only achieves π in the limit as $z \to \infty$. So $\pi \geq \phi > \theta$. $\square$

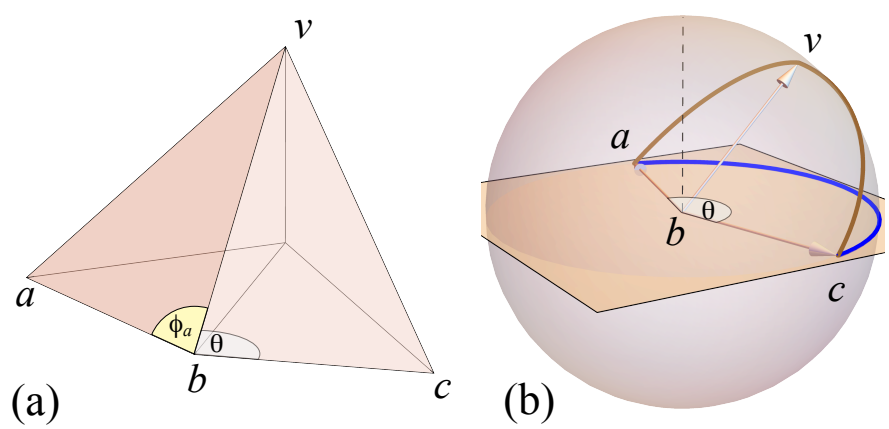

Figure 3: (a) Convex angle θ at b in the plane, angles ϕ_a and ϕ_c above the plane. (b) θ is the length of the blue arc on $\mathbb{S}$, shorter than the sum of the ϕ_a and ϕ_c arcs (brown).

Lemma 2 *If the degree of vertex* b *is greater than* 3*, so that there are a series of* $v_i b$ *edges incident to* b*, with* $v_1, \ldots, v_k$ *forming a convex chain, the opening conclusion of Lemma 1 still holds.*

Proof: The reason to require $v_1, \ldots, v_k$ to form a convex chain (lie on the convex hull with a, b, c) is that a zigzag chain could open beyond π.

Let ϕ be the sum of the angles above the plane incident to b. The triangle inequality on $\mathbb{S}$ used in Lemma 1 still holds, for arc $\vec{a}\,\vec{c} = \theta$ is a geodesic of length $\leq \pi$, and a non-geodesic path

$$\vec{a}\,\vec{v_1},\ \vec{v_1}\,\vec{v_2}, \ldots, \vec{v_k}\,\vec{c}$$

will be longer.

This establishes that $\phi > \theta$: ϕ is an opening of θ. □

Opening from the Reflex Side. Let L_B and L_A be the B- and A-sides of L respectively, closed polygonal chains (open chains after the safe-cut). Lemmas 1 and 2 apply to L_B: a convex chain opened from the convex side.

However, L_A is a convex chain opened from the reflex side as z increases. Fortunately, it does not matter from which side the opening is initiated:

Lemma 3 *The 3D angle ϕ opens the convex chain the same amount from v_i on the convex side as on the reflex side.*

Proof: Again let the planar angle $\angle a, b, c$ be θ, opened to ϕ by v on the convex side. We first argue for b having degree-3 and generalize to arbitrary degree later.

Reflect v to v' so that $v_0 v_0'$ is a straight segment through b. See Fig. 4(a). We claim that $\phi_a = \angle a, b, v$ plus $\phi_a' = \angle a, b, v'$ is exactly π, and similarly $\phi_c + \phi_c' = \pi$, and therefore $\phi + \phi' = 2\pi$. This claim is established via the Gaussian sphere $\mathbb{S}$.

Consider Fig. 4(b). The claim for $\phi_c + \phi_c' = \pi$ translates to the two blue arcs, from $\vec{v}$ to $\vec{c}$ and from $\vec{v'}$ to $\vec{c}$, summing to π. This can be seen by reflecting c through the origin b to $c' = -c$, when it is now clear that $\vec{v'}$ to $\vec{c'}$ completes the arc from $\vec{c}$ to $\vec{v'}$ to $\vec{c'}$.

Now the opening from v on the convex side is $\phi - \theta$—3D angle minus planar angle—while the opening from v' on the reflex side is

$$\begin{aligned} &= \phi' - (2\pi - \theta) \\ &= (2\pi - \phi) - (2\pi - \theta) \\ &= \phi - \theta \end{aligned}$$

Clearly this argument works for several segments $v_i b$ incident to v. □

Lemma 4 *The opening in Lemmas 1 and 2 is monotonic as a function of the z-coordinates of the v_i.*

From the Gaussian sphere viewpoint, it is intuitively clear that increasing z increases the sum of the arc lengths, as increasing z moves the $\vec{v_i}$ closer to vertical, further away from the θ are in the plane. But I have not found a convincing geometric proof.

Proof: If b has degree-3 (one edge vb incident to b, then one can explicitly calculate $\phi(z)$ and use calculus to show that $\phi(z)$ increases with z. See below for the equations.

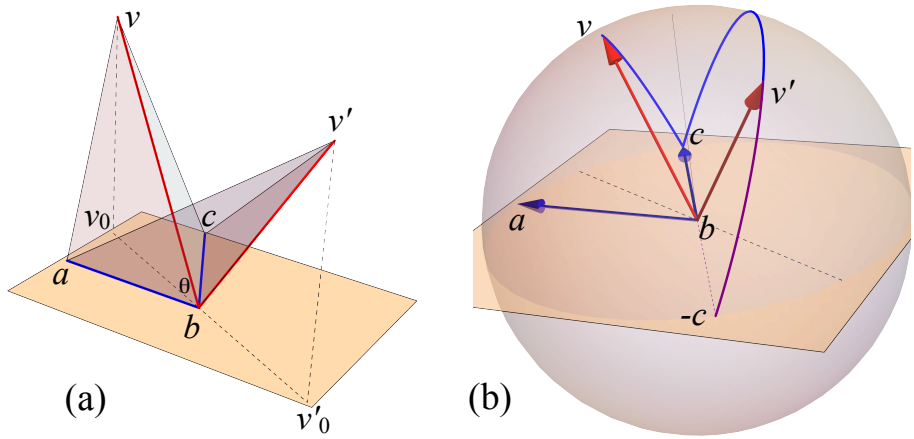

Figure 4: (a) v reflected to v'. (b) $\vec{c}$ to $\vec{v'}$ (blue) to $\vec{c'}$ (Purple) is half a great circle, of length π.

If b has degree greater than 3, then treat each v_i separately, with ϕ_a the angle $\angle v_i, b, v_{i-1}$ and ϕ_c the angle $\angle v_i, b, v_{i+1}$ Since the sum of individually increasing angles is itself increasing, the same analysis for degree-3 holds.

□

Explicit Equations. Choosing coordinates wlog

$$(a, b, c) = ((-1, 0, 0), (0, 0, 0), (\cos(\pi - \theta), \sin(\pi - \theta), z)\ ,\ 0 < \theta < \pi$$

and $v = (x, y, z)$, then ϕ can be expressed explicitly:

$$\phi(z) = \arccos\left(\frac{-x}{\sqrt{x^2 + y^2 + z^2}}\right) + \arccos\left(\frac{-x\cos\theta + y\sin\theta}{\sqrt{x^2 + y^2 + z^2}}\right)\ .$$

A typical evaluation shows that indeed $\phi(z)$ equals θ when $z = 0$ and then increases toward π for $z > 0$: see Fig. 5.
The derivative with respect to z is:

$$\frac{\partial\phi(z)}{z} = z\left(-\frac{x}{\sqrt{1 - \frac{x^2}{x^2+y^2+z^2}}} + \frac{-x\cos\theta + y\sin\theta}{\sqrt{1 - \frac{(-x\cos\theta + y\sin\theta)^2}{x^2+y^2+z^2}}}\right)$$

A tedious analysis of this expression shows that it is ≥ 0, and so $\phi(z)$ grows monotonically with z.

3.1 Opening Summary

Theorem 2 *Let ρ_0 and ρ_z be two planar convex polygonal chains forming a convex triangulated band between them, as illustrated in Fig. 6. Then leaving ρ_0*

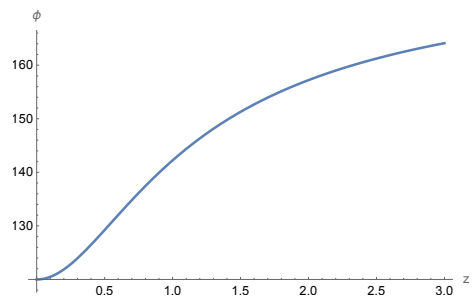

Figure 5: $\phi(z)$ when $(\theta, x, y) = (120°, 0, 1)$.

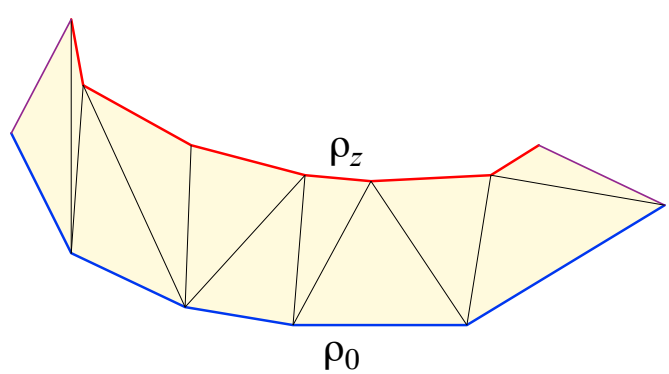

Figure 6: Two planar convex chains determining a convex band.

in the plane while orthogonally lifting every vertex of ρ_z to the same height z above the plane, opens the ρ_0 chain, opens in the sense that the planar angle θ at a ρ_0 vertex. increases to $\phi > \theta$ while remaining convex, $\pi > \phi$.

The same holds true if we reverse the roles, leaving ρ_x in the plane while lifting ρ_0.

Finally, the opening is monotonic with z.

Proof: Lemma 1 establishes the claim for a vertex of ρ_0 of degree-3, i.e., incident to only one triangulation diagonal. Lemma 2 extends the result to a vertex of arbitrary degree.

Lemma 3 shows that viewing the chains as reflex, reversing the roles of the two chains, leads to the same conclusion.

Finally, Lemma 4 establishes that the opening is monotonic with z: the angle $\phi(z)$ at a vertex increases with z. □

Of course in our case the two chains are L_B and L_A bounding the band L.

4 Radial Monotonicity

Now that we know that increasing the z-height of A opens both the polygonal chain boundaries L_B and L_A of the band, we turn to placing B and A along those boundaries to ensure nonoverlap.

We will show that the hexagon A in Fig. 1 is essentially the only shape for which A cannot be safely placed. We will define a class of shapes that do permit safe placement.

This class of shapes is defined using the concept of radial monotonicity, introduced in [O'R16] and subsequently used in [O'R18] and in [Rad24]. Opening a radially monotone path avoids crossings between the two sides of the path; see ahead to Fig. 9. A path that is not radially monotone always allows an opening that self-crosses: see Fig. 7.

An open, directed polygonal chain ρ with start endpoint v is ***radially monotone with respect to v*** (RM_v) if every circle centered on v meets ρ in a single point. A chain is ***radially monotone*** without qualification (RM) if it is radially monotone with respect to each of its vertices. We first establish this easily proved lemma:

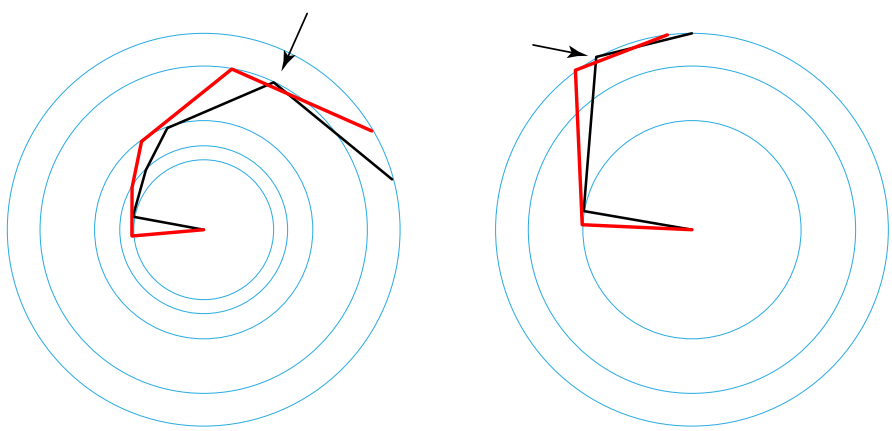

Figure 7: Violation of RM leads to crossing. Here only $\omega_1 > 0$. Note, all angles α_i are obtuse.

Lemma 5 *Acute $\Rightarrow \neg$RM: A polygonal chain ρ with an acute angle α_i at some internal vertex v_i is not RM.*

Proof: Consider the circle centered on v_{i-1} with radius $|v_{i-1}v_i|$. Then RM is violated at v_i. Because RM means radial monotonicity from every vertex, and it is violated at v_i, ρ is not RM. □

Note convexity is not needed for this lemma's claim. In contrast to the lemma, a polygonal chain ρ with all angles α_i obtuse might or might not be RM. See Fig. 7.

The RM concept has not been studied for convex RM chains. In general, RM_v does not imply RM, but for convex ρ, it does. This simplifies further analysis.

Lemma 6 *For convex ρ, $RM_v \Rightarrow RM$: radial monotonicity with respect to one vertex v implies radial monotonicity for all vertices beyond v.*

Proof: Let polygonal chain ρ be RM_v, where $v = v_1$ is its first vertex. Assume ρ is convex bending clockwise. Suppose in contradiction to the claim of the lemma that ρ fails to be RM at vertex v_i, with a RM violation occurring at vertex v_j. See Fig. 8.

To violate RM at v_j means that ρ continues beyond v_j penetrating the circle C (brown in the figure) centered on v_i of radius $|v_i v_j|$. Because ρ is convex, this violation must occur clockwise of the (red) tangent to C; counterclockwise of the (dashed) tangent would introduce a nonconvexity. But such a continuation violates MR_v, contradicting our assumption. □

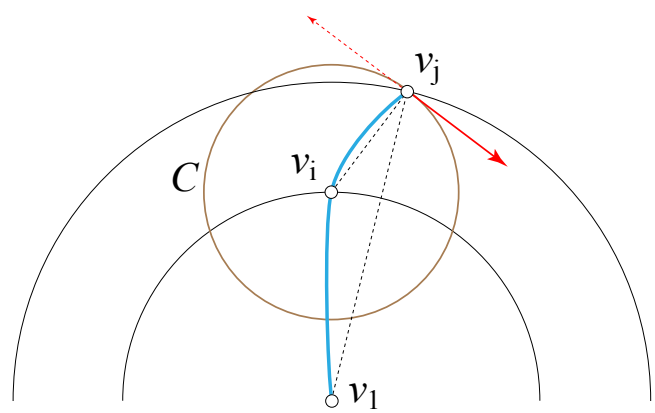

Figure 8: For convex ρ (blue), RM with respect to v_1 implies RM_{v_i}.

An ***opening*** of a convex polygonal chain increases (or leaves unchanged) each internal angle, opened not more than π. The key property is opening an RM-chain avoids self-intersection. Notation: Let ρ be a convex chain curling cw, $\alpha_i \leq \pi$ the convex angle at vertex v_i, and $\omega_i \geq 0$ the amount that α_i is opened.

Lemma 7 *Let ρ be a radially monotone convex polygonal chain, reindexed (if necessary) so that v_1 is the first vertex at which $\omega_i > 0$. Then for ρ^o, an opened version of ρ, $\rho \cap \rho^o = \{v_1\}$, the common first vertex.*

First we should note that this follows from Cauchy's Arm Lemma, in particular, from Corollary 4 of [O'R01]: "a valid reconfiguration of an open convex chain remains simple." In our case, a valid reconfiguration is just an opening.

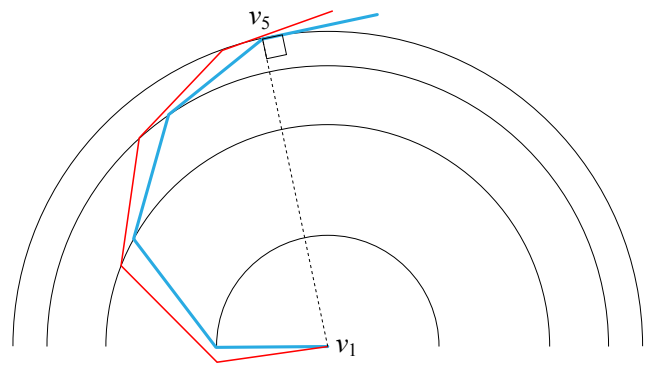

Figure 9: A radially monotone path ρ (blue) opened at v_1. The last link v_5v_6 is tangent to the circle through v_5. Each segment remains in its annulus as ρ is opened.

Nevertheless, we need a more detailed understanding of this centrally important chain opening, and so we offer two arguments.

Proof: Let ρ_1 be the chain ρ opened by ω_1 at v_1, with all other $\omega_i = 0$. Because ρ is radially monotone, ρ_1 does not touch ρ except at v_1, as illustrated in Fig. 9: each segment of ρ remains within its annulus..

Now let v_i be the next vertex at which $\omega_i > 0$, and let v_i' be the position of v_1 after the opening at v_1 by ω_1 See Fig. 10.

Then opening v_i' by ω_i rotates the suffix chain ccw about v_i', with each segment remaining within its annulus centered on v_i'. Because the rotation is ccw, it moves the chain further away from ρ, avoiding intersection.

Continuing in this manner, each subsequent opening further along the chain sweeps ccw away from the initial ρ. So $\rho \cap \rho^o = \{v_1\}$.

For an alternative proof by induction, note that for a chain consisting of a single edge, the claim is obvious. Assume now that the claim holds for all chains of length k, and consider a chain ρ of length $k+1$. Open ρ from v_2 onward using the induction hypothesis. This results in a chain ρ' that satisfies $\rho \cap \rho' = \{v_2\}$. Now open v_1 by ω_1, producing ρ^o. As each segment of ρ moves ccw within its annulus, intersections are avoided and $\rho \cap \rho^o = \{v_1\}$. $\square$

A final remark for intuition. The opened chain ρ^o lies within the ***involute region*** bounded by the involute of the chain. See Fig. 11.

It is easy to see that an opening of a RM path is itself RM. This helps justify the continuous Lemma 4.

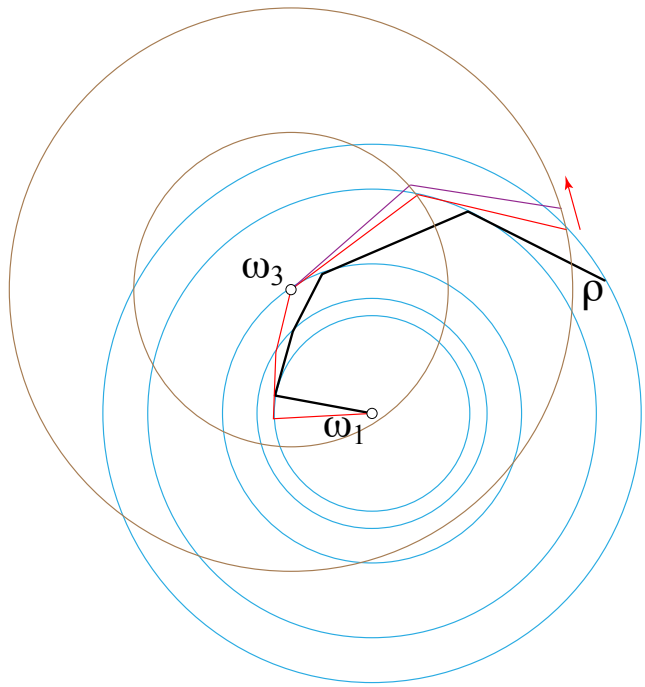

Figure 10: The opening of ρ by $\omega_3 > 0$ at v_3 sweeps ccw away from ρ.

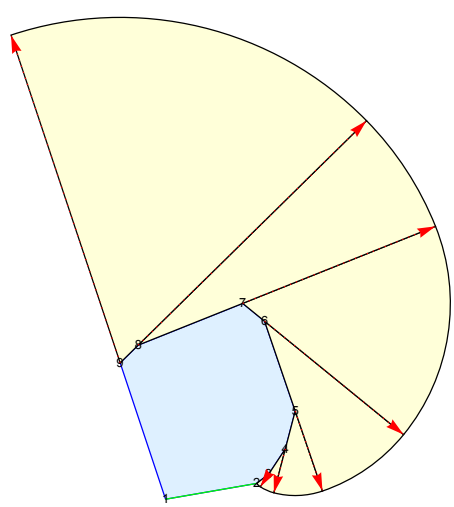

Figure 11: The involute of a convex chain tracks the unspooling of a taut string.

5 Polygons with the RM-property

Say that a convex polygon P with ccw oriented ∂P has the ***RM-property***, if it has an edge $e = (a, b)$ and a vertex c so that the cw path of P from a to c is RM, and the ccw path of P from b to c is RM. We'll call c the ***apex vertex*** of the RM-property.

As a simple example, every regular polygon P has the RM-property, as we now show. Let e be the "middle edge" of P. When n is odd, there are equal paths to either side of e. For n even one side is one link longer than the other side. We claim without proof that these paths to either side of e are radially monotone.

Why the RM-property. We need no constraints on the shape of B, as it will safely attach to the reflex side L_B of the unfolded band, as in Fig. 2(b). But A is surrounded by the band and must attach to the convex side L_A. Note the edges of L_A are in one-to-one correspondence to the edges of A.

Lemma 8 *Let A have the RM-property with respect to $e = (a, b)$ and apex vertex c. If A attaches its edge e to the corresponding edge of L_A, and there is a safe cut from v, then A does not overlap band L for all z-heights of A.*

Proof: Let the a-chain be the chain of edges cw from a to c and the b-chain be the chain of edges ccw from b to c. See Fig. 12.

Lemma 7 guarantees that opening the a-chain avoids intersection with the original a-chain, and similarly the b-chain. It only remains to show that the a-chain does not intersect the b-chain.

This follows by composition of rotations, a topic originally studied by Euler. Proposition 9 states that the composition leads to rotation about a point in the convex hull of the individual rotations. As can be seen in Fig. 12, this guarantees that the motions of the cut point c "spread" at c, to the left and right of the perpendiculars at c. (Note these perpendiculars are the start vectors of the involutes described in Fig. 11.) Therefore A does not overlap the band boundary L_A for opening caused by any z. $\square$

Proposition 9 *n planar rotations about centers v_i by angle ω_i, where $\sum \omega_i \leq \pi$, are equivalent to a single rotation about a point p, where center p is a weighted sum of the v_i, weighted by ω_i. Moreover, p is in the convex hull of the v_i.*

6 Band Unfolding Examples

To supplement the example shown earlier in Fig. 2, here we include a few more. Fig. 13 illustrates the effect of increasing z.

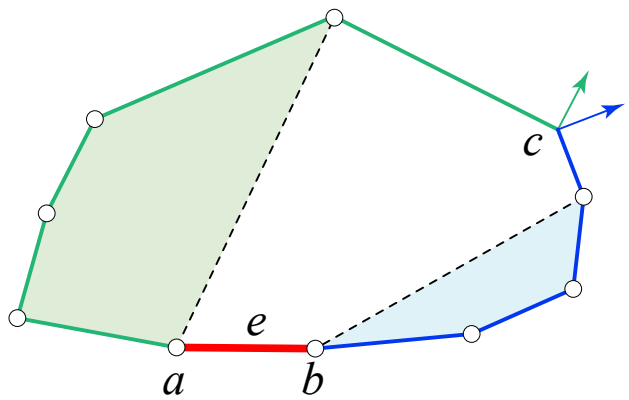

Figure 12: The RM-property with respect to $e = (a, b)$ and apex c. The shaded regions show the convex hulls of the left and right centers of rotation.

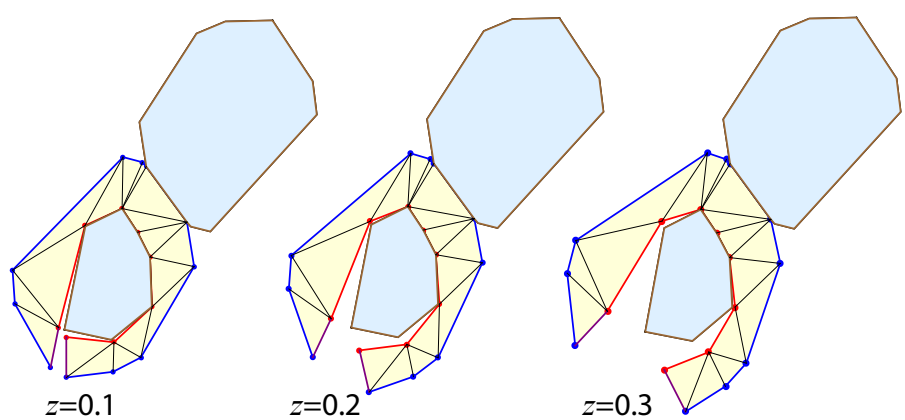

Figure 13: Three different z-heights for same example.

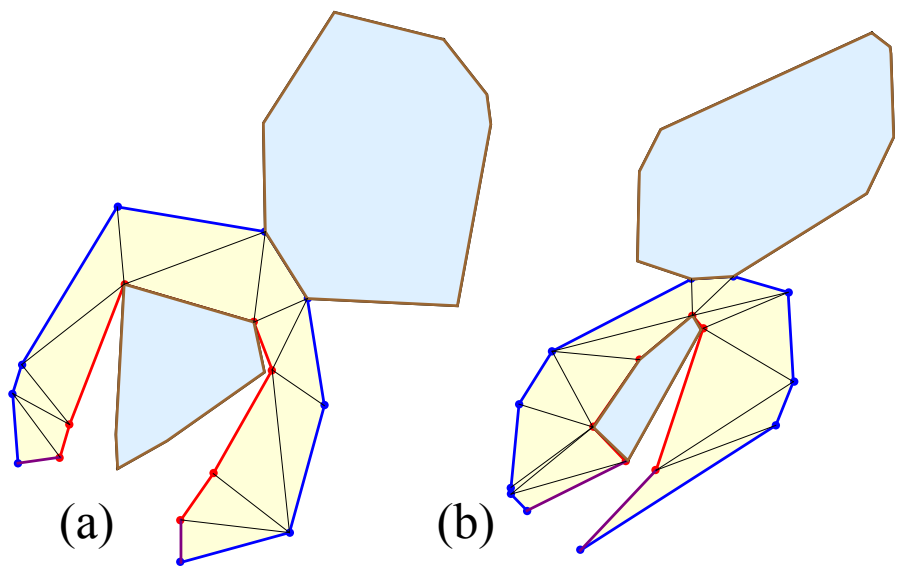

Figure 14: Two random examples, both $z = 0.2$. (a) $n_A = 6$, (b) $n_A = 5$.

7 RM-property Examples

Fig. 15 shows that the RM-property is common. In fact, it is only shapes

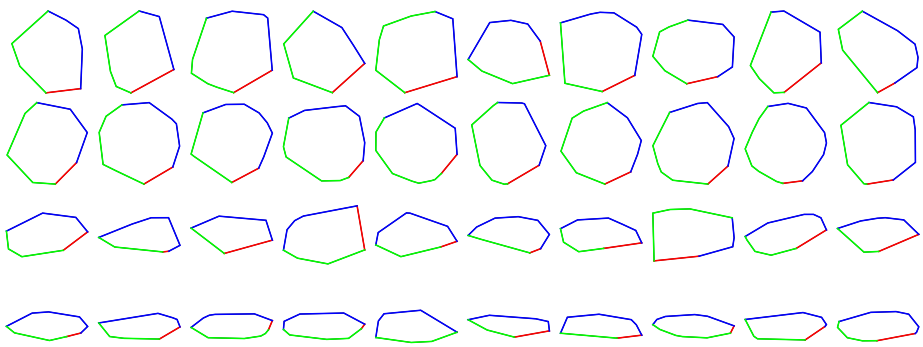

Figure 15: Forty random polygons each with the RM-property with respect to its red edge: Right chain blue, left chain green.

essentially like the counterexample shown earlier in Fig. 1 that lead to overlap. Fig. 16 shows why such shapes fail to have the RM-property: they necessarily contain an acute angle, and so are not RM by Lemma 5.

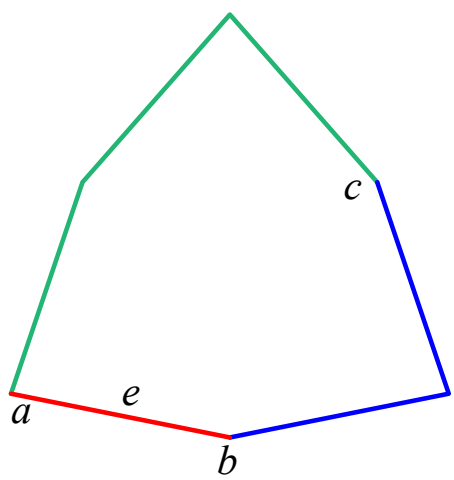

Figure 16: Hexagonal polygon that does not have the RM-property. Both left and right chains (cw a to c and ccw b to c) are not RM.

And if a polygon A fails to have the RM-property, then there is some prismatoid with top A whose band-unfolding self-overlaps. This is because an overlap violation occurs immediately upon any amount of opening; see Fig. 7. So Theorem 1 completely characterizes when band-unfolding is possible.

8 Open Problems

(1) Is there a safe-cut for the band of every nested prismatoid? (This is only known to hold for nested prismoids.)

(2) Can the z-lifting proof be extended to handle nested "layer-cake" polyhedra? Here I am defining a ***nested layer-cake polyhedron*** as a stack of nested prismatoids.

(3) Does every non-nested prismatoid have an edge-unfolding? This central open problem remains unresolved.

References

[ADL+08] Greg Aloupis, Erik D. Demaine, Stefan Langermann, Pat Morin, Joseph O'Rourke, Ileana Streinu, and Godfried Toussaint. Edge-unfolding nested polyhedral bands. *Comput. Geom. Theory Appl.*, 39:30–42, 2008.

[O'R01] Joseph O'Rourke. An extension of Cauchy's arm lemma with application to curve development. In *Proc. 2000 Japan Conf. Discrete Comput. Geom.*, volume 2098 of *Lecture Notes Comput. Sci.*, pages 280–291. Springer-Verlag, 2001.

[O'R07] Joseph O'Rourke. Band unfoldings and prismatoids: A counterexample. Technical Report 087, Smith College, October 2007. arXiv:0710.0811v2 [cs.CG]; http://arxiv.org/abs/0710.0811.

[O'R13a] Joseph O'Rourke. Dürer's problem. In Marjorie Senechal, editor, *Shaping Space: Exploring Polyhedra in Nature, Art, and the Geometrical Imagination*, pages 77–86. Springer, 2013.

[O'R13b] Joseph O'Rourke. Unfolding face-neighborhood convex patches: Counterexamples and positive results. In *Proc. 25th Canad. Conf. Comput. Geom.*, pages 79–84, August 2013. Full version includes 6-page Appendix. Precursor: arXiv:1205.2048 [cs.CG].

[O'R16] Joseph O'Rourke. Unfolding convex polyhedra via radially monotone cut trees. *arXiv:1607.07421*, 2016. https://arxiv.org/abs/1607.07421.

[O'R18] Joseph O'Rourke. Edge-unfolding nearly flat convex caps. In *Proc. Symp. Comput. Geom. (SoCG)*, volume 99, pages 64:1–64:14. Leibniz Internat. Proc. Informatics, June 2018.

[Rad24] Manuel Radons. Edge-unfolding nested prismatoids. *Comput. Geom.*, 116:102033, 2024.